International Journal of Applied Pharmaceutics

ISSN- 0975-7058 Vol 14, Special Issue 4, 2022

Original Article

PHARMACOKINETIC PREDICTIONS AND MOLECULAR DYNAMIC ANALYSIS OF TERPENOID AND FLAVONOID COMPOUNDS FROM MIANA LEAVES (*PLECTRANTHUS SCUTELLARIOIDES* (L.) R. BR.) AS AN ANTIMALARIAL CANDIDATES ON PLASMEPSIN II RECEPTOR

AMI TJITRARESMI[1*], KIRKA DWI APRIALI[1], KAMILA NURVIANITA[1], IDA MUSFIROH[2], MOELYONO MOEKTIWARDOYO[1], YASMIWAR SUSILAWATI[1]**

[1]Department of Pharmaceutical Biology, Faculty of Pharmacy, Universitas Padjadjaran, Sumedang 45363, Indonesia, [2]Department of Pharmaceutical Analysis and Medicinal Chemistry, Faculty of Pharmacy, Universitas Padjadjaran, Sumedang 45363, Indonesia

*Email: ami.tjitraresmi@unpad.ac.id

Received: 18 Jul 2022, Revised and Accepted: 23 Aug 2022

ABSTRACT

Objective: This study aims to find antimalarial candidates from 32 terpenoids and three flavonoid compounds found in miana leaves *in silico* using plasmepsin protein as a receptor through docking simulations, molecular dynamics simulations, and pharmacokinetic predictions.

Methods: The research was conducted *in silico* through molecular docking simulation, molecular dynamic simulations, analysis of potential compounds using Lipinski's rule, and prediction of ADMET based on ligands.

Results: The results showed isophytol had the best interaction with the plasmepsin II based on the low free binding energy (FBE) and led to hydrogen bonding with the plasmepsin II crucial amino acid, Asp34. Isophytol has the best result in molecular dynamic simulation. Based on pharmacokinetics predictions, toxicity, and Lipinski's rule of five, most tested compounds, including isophytol, meet the criteria as a promising drug.

Conclusion: Isophytol from miana leaves with plasmepsin II protein has the best and most stable interaction based on the results of molecular dynamic simulation, so this compound was a candidate for antimalarial drugs.

Keywords: Miana, *In silico*, Malaria, Plasmepsin II

DOI: https://dx.doi.org/10.22159/ijap.2022.v14s4.PP35 Journal homepage: https://innovareacademics.in/journals/index.php/ijap

INTRODUCTION

Malaria remains a significant public health problem. Based on WHO 2019 data, there were 299 million cases with 409 thousand deaths due to malaria Malaria is caused by a Plasmodium protozoan parasite transmitted to humans by infected Anopheles mosquitos [1]. There are four Plasmodium types: *Plasmodium ovale*, *Plasmodium falciparum*, *Plasmodium vivax*, and *Plasmodium malariae*. The most virulent form of the parasite is *Plasmodium falciparum* [2]. The emergence of *Plasmodium falciparum* strains resistant to antimalarial drugs necessitates identifying and developing new drug targets in malaria control. Antimalarial drug resistance is caused by mutations or biochemical changes in the target drug's active site [3-6].

In the erythrocytic phase, Plasmodium reproduces in the human body by consuming hemoglobin. Hemoglobin is digested in the food vacuole of the parasite with the help of protease enzymes. Three types of protease enzymes found in the food vacuole of the malaria parasite are falcilysin (metalloprotease), falcipain (cysteine protease), and plasmepsin (aspartic protease) [7, 8]. Plasmepsins are recognized as crucial enzymes of the three enzymes involved in Hb digestion as they break down Hb catalytically, so these enzymes are sought as potential drug targets. Plasmepsin (plasmodium pepsin) is essential in every stage of plasmodium development in the host body. Four types of plasmepsin (plasmepsin I, plasmepsin II, plasmepsin IV, and histo-aspartic protease (HAP)), referred to as digestive plasmepsin, are present in the food vacuole of parasites and are involved in the degradation of hemoglobin [9, 11]. Plasmepsin I and plasmepsin II II are elaborate in the degradation stage of hemoglobin, while plasmepsin IV and HAP work to digest hemoglobin and degrade the products of hemoglobin degradation of phase I and its initial into shorter peptides. Plasmepsin II is an effective drug target for the treatment of malaria. Plasmepsin II consists of 329 amino acids and is folded into two topologically similar domains, N-and C-terminal. The binding slot on plasmepsin II contains Asp34 and Asp 214, catalytic dyads. The plasmepsin II inhibitors are characterized by a hydroxyl group that displaces the catalytic water molecule at the active site, forming hydrogen bonds with catalytic Asp34 and Asp214 [10-12].

Miana is a plant of the genus Plectranthus, family Lamiaceae. Indonesian people have used miana leaves (*Plectranthus scutellarioides* (L.) R. Br.) as antimalarial drugs. In North Sulawesi, miana leaves are used as malaria therapy with a mixture of betel leaf (*Piper betle* Linn.), honey, and eggs [13]. Plants from the Lamiaceae family have been proven to be sources of plants that have antimalarial activity [14].

Previous researchers have isolated compounds from miana leaves, and most of these compounds belong to the terpenoid and flavonoid groups [15-20]. However, the active antimalarial compounds from miana leaves are not yet known. The *in silico* study was conducted first to save time and cost. This study will identify secondary metabolites of miana leaves that have antimalarial activity against the plasmepsin II enzyme through molecular docking, molecular dynamic approach simulations, and pharmacokinetic predictions.

MATERIALS AND METHODS

Hardware and software

The hardware used in this research was a set of personal computers with the following specifications: Intel® Core™ i5-8250U CPU @1.60GHz (8 CPUs), NVIDIA GeForce MX130, 256 GB SSD, 1 TB HDD and 8GB DDR4 RAM.

Software used for this research were ChemDraw Ultra 12.0, Chem3D 12.0, Molegro Molecular Viewer 2.5, Autodock 4.2.6, AutoDockTools 1.5.6, BIOVIA Discovery Studio 2021, and several web server programs such as PdbSum, pkCSM, ADMETlab 2.0, and RCSB PDB.

Preparation of ligands

Ligands used for this study were 32 terpenoids (neomenthol; linalool; germacrene-D; neophytadiene; delta-cadinene; alpha-

humulene; 6, 10, 14-trimethyl-2-pentadecanone; copaene; caryophyllene oxide; alpha-selinene; alpha-cadinol; beta-sesquiphellandrene; aromadendrene; nerolidol; alpha-calacorene; torreyol; alpha-cubebene; beta-caryophyllene; isophytol [18]; spiroscutelone A; spiroscutelone B; spiroscutelone C [17]; scutellarioidone A; scutellarioidone B; scutellarioidone C; 6-acetylfredericone B; scutellarioidone D; scutellarioidolide A; coleon O; coleon G; lanugone K; fredericone B [15]) and 3 flavonoids compounds (apigenin-5-O-(3′′-O-acetyl)-B-D-glucuronide; apigenin-7-O-(3′′-O-acetyl)-B-D-glucuronide [16]; quercetin [20]) from miana leaves. Artemisinin was selected as a positive control. The ligands were built in 2D using the ChemDraw Ultra 12.0 program, then converted into 3D and minimized energy using Chem3D. The ligands were protonated to produce a pH of 7.4 and the structural conformation was determined by conducting conformational explorations [21].

Preparation of receptors

The receptor of this research was plasmepsin II which can be downloaded via the Protein Data Bank (http://www.rcsb.org/) with the PDB code: 2IGY. The receptor was separated from its native ligand (A2T) and water molecules using BIOVIA Discovery Studio. Then polar hydrogen atoms were added using AutoDockTools and a Kollman charge so that they could bind to the ligands.

Molecular docking and visualization

Molecular docking was performed using AutoDockTools to determine the affinity of protein-ligand-binding interactions using the Lamarckian genetic algorithm with a population size of 100 individuals. The docking parameters were validated by redocking the native ligand to its previously separated receptor using the validation parameter, RMSD 2.0 Å[5], [22]. Visualization was presented to determine the ligand-receptor interactions in 2D and 3D forms. The best dock results were used to create complex files for visualization using BIOVIA Discovery Studio 2021.

Screening ligand-based drugs likeness (drug scan)

Lipinski's rule of five of the docking compounds was calculated by web pkCSM (http://biosig.unimelb.edu.au/pkcsm/prediction). These parameters include log P ≤5, molecular weight ≤500 g/mol, hydrogen bond donor ≤5, and hydrogen bond acceptor ≤10 [23].

Pharmacokinetics and toxicity predictions

Analysis of pharmacokinetic properties of secondary metabolites of miana leaves was used using a web pkCSM (http://biosig.unimelb.edu.au/pkcsm/prediction) and ADMETlab 2.0 program (https://admetmesh.scbdd.com/service/evaluation/index). The parameters analyzed were Human Intestinal Absorption (HIA) and Caco2 cells for absorption, Plasma Protein Binding (PPB) and Blood Brain Barrier (BBB) for distribution, CYP inhibitors for metabolism, and Ames Toxicity for mutagenicity and carcinogenicity.

Molecular dynamics simulation

The terpenoid and flavonoid compounds from miana with the lowest FEB were subjected to Molecular Dynamics (MD) simulations. The MD simulations were conducted using the AMBER ff14SB force field for proteins. The substances were exposed to the General AMBER force field (GAFF), and TIP3P water was attached to the 10x10x10 box. Topology files were created (RESP) after the ligands were neutralized with electrostatic potential. Amber16's Sander module was utilized for minimization, heating, and equilibration. A dynamic simulation uses a heating system to admit the ligands and receptors interacting with previously specified force fields before entering the molecular production stage. The heating process was done in three steps, (1) heating from 0 to 310 K; (2) heating at regular intervals; (3) heating to approximate the physiological temperature of the body. The system is then equilibrated to return to a constant state before performing molecular dynamics simulations. The MD results can calculate the Root Mean Square Deviation (RMSD) and Root Mean Square Fluctuation (RMSF) [24].

RESULTS

The macromolecular structure of the plasmepsin II receptor with PDB ID: 2IGY is the crystal structure of the receptor on *Plasmodium falciparum* organisms obtained by X-ray diffraction with a resolution value of 2.60. Fig. 1 showed the redocking validation of the 21GY receptor with a grid box size of 30 x 34 x 30 and x, y, and z coordinates (42.688;-4.605; and-11.522) for the A2T ligand yielding an RMSD value of 0.872 Å. Based on the docking results for A2T-plasmepsin II (2IGY), the amino acids responsible for A2T (native ligand) binding at the plasmepsin II binding site are Tyr77, Asp34, Gly36, and Thr217, form carbon-hydrogen bond interactions, and Trp41, Phe111, Tyr115, Ile300, Ile32, Tyr192, and Met15 form hydrophobic interaction.

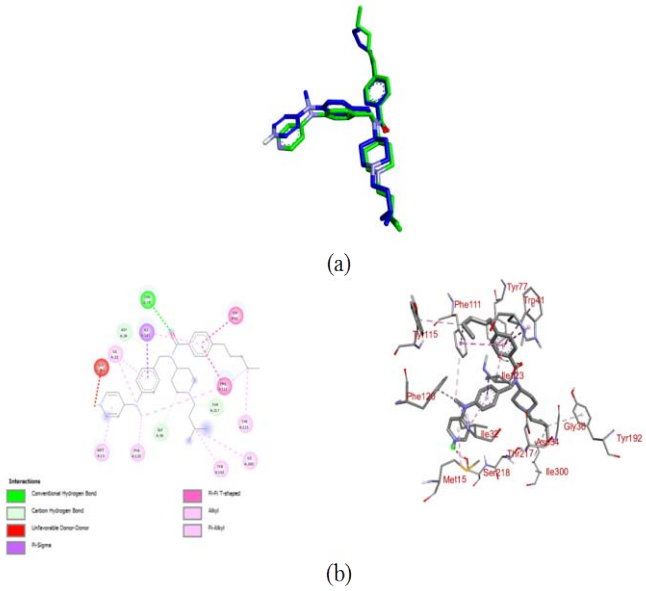

Fig. 1: Overlay conformation of A2T-plasmepsin II (2IGY) validated results (blue) and A2T-plasmepsin II (2IGY) crystallographic results (green) (a) and the 2D and 3D visualization of A2T-plasmepsin II (2IGY) docking results (b), table 1 shows the docking results of 35 miana leaf compounds as ligands in plasmepsin II (2IGY) as an enzyme receptor

Table 1: **Docking results of miana leaf compounds in plasmepsin II enzyme receptors**

No	Compounds	Pubchem ID	Δ°G (kcal/mol)	Ki (μM)	Amino acid interaction	
					Hydrogen binding	Hydrophobic binding
	Artemisinin ($C_{15}H_{22}O_5$)	68827	-6.32	23.15	Ser37	Ile32, Met75, Ile123, Val82
1	Neomenthol ($C_{10}H_{20}O$)	439263	-5.44	103.72	Try 77	Trp41, Phe111, Ile123, Met75, Val82
2	Linalool ($C_{10}H_{18}O$)	6549	-4.51	494.51	-	Ile123, Try77, Met75, Trp41, Val82, Try115, Phe111
3	Germacrene-d ($C_{15}H_{24}$)	91723653	-6.48	17.67	-	Phe111, Val82, Tyr77, Met75, Trp41, Ile123
4	Neophytadiene ($C_{20}H_{38}$)	10446	-4.92	246.54	-	Tyr77, Ile123, Phe111, Met75, Ile32, Phe120, Trp41
5	Delta-cadinene ($C_{15}H_{24}$)	441005	-6.42	19.62	-	Ile123, Met75, Val82, Trp41, Phe111
6	Alpha-humulene ($C_{15}H_{24}$)	5281520	-5.51	90.77	-	Phe111, Tyr77, Ile123, Met75, Trp41
7	6, 10, 14-trimethyl-2-pentadecanone ($C_{15}H_{24}O$)	10408	-4.96	233.26	Ser118	Try77, Ile123, Phe111, Met75
8	Copaene ($C_{15}H_{24}$)	12303902	-8.09	1.18	-	Ile123, Met75, Tyr77, Val82, Trp41, Phe111
9	Cariophyllene oxide ($C_{15}H_{24}O$)	1742210	-5.94	44.22	Tyr77	Ile123, Val82, Trp41, Met75, Phe111
10	Alpha-selinene ($C_{15}H_{24}$)	10856614	-7.81	1.88	-	Trp41, Ile123, Val82, Val105, Met75, Phe111, Tyr77
11	Alpha-cadinol ($C_{15}H_{26}O$)	10398656	-6.06	36.09	Trp41	Ile123, Val82, Tyr77, Phe111
12	Beta-sesquiphellandrene ($C_{15}H_{24}$)	12315492	-7.18	5.44	-	Trp41, Met75, Ile123, Val82, Val105, Tyr115, Phe111
13	Aromadendrene ($C_{15}H_{24}$)	91354	-6.39	20.59	-	Phe111, Tyr77, Ile123, Met75, Trp41
14	Nerolidol ($C_{15}H_{24}O$)	5284507	-6.32	23.47	Asp34	Trp41, Phe111, Tyr77, Val82, Ile123, Met75, Tyr115
15	Alpha-calacorene ($C_{15}H_{20}$)	12302243	-7.21	5.22	-	Tyr77, Ile123, Trp41, Phe111
16	Torreyol ($C_{15}H_{26}O$)	3084311	-6.11	33.01	Asp34	Trp41, Ile123, Val82, Phe111
17	Alpha-cubebene ($C_{15}H_{24}$)	442359	-6.24	26.65	-	Val82, Met75, Trp41, Ile123, Tyr77, Phe111
18	Beta-caryophyllene ($C_{15}H_{24}$)	5281515	-6.01	39.26	-	Ile123, Val82, Met75, Phe111, Tyr 7, Trp41
19	Isophytol ($C_{20}H_{40}O$)	10453	-6.45	18.85	Asp34	Trp41, Ile32, Phe111, Met75, Val82, Ile123
20	Spiroscutelone A ($C_{24}H_{30}O_9$)	-	-6.73	11.62	Gly216	-
21	Spiroscutelone B ($C_{24}H_{30}O_9$)	-	-5.76	59.69	Ser218, Tyr77, Asp214, Thr217	Phe111
22	Spiroscutelone C ($C_{26}H_{34}O_{10}$)	-	-5.76	38.09	Tyr77, Thr217, Gly216, Asp214	Phe111, Ile32
23	Scutellarioidone A ($C_{20}H_{26}O_7$)	-	-4.62	407.59	Ile173, Asn151	Ile123, Val82
24	Scutellarioidone B ($C_{24}H_{30}O_9$)	-	-4.82	294.08	Ile173, Ser319, Asn317	Tyr184, Leu153
25	Scutellarioidone C ($C_{24}H_{28}O_9$)	-	-4.48	518.31	Tyr184, Asp314, Asn317	Val312, Tyr184, Leu153
26	6-Acetylfredericone B ($C_{24}H_{32}O_6$)	-	-5.38	114.76	Ser319, Asn317, Tyr184	Ile173
27	Scutellarioidone D ($C_{22}H_{28}O_6$)	-	-4.68	369.78	Ile173, Asp314	Asp314, Leu153
28	Scutellarioidolide A ($C_{26}H_{34}O_8$)	-	-5.66	70.76	Tyr77, Thr114, Thr217	Ile123, Ile32, Met15
29	Coleon O ($C_{22}H_{28}O_6$)	162790	-5.79	57.2	Ser218	Phe120, Phe111, Ile123, Ile32, Met15
30	Coleon G ($C_{22}H_{28}O_6$)	98125349	-6.37	21.4	Gly216, Ser218, Ser118	Ile123, Ile32, Phe111
31	Lanugone K ($C_{22}H_{30}O_6$)	-	-5.95	43.67	Ser218	Ile32, Phe120, Phe111, Met15, Ile14
32	Fredericone B ($C_{22}H_{28}O_6$)	-	-6.87	9.24	Asp34, Gly216, Gly36	Ile123, Ile32, Phe111, Tyr77
33	Apigenin 5-O-(3′′-O-Acetyl)-B-D-Glucuronide ($C_{23}H_{20}O_{12}$)	-	-5.76	215.25	Asp34, Tyr77, Ser218, Gly216, Tyr17	Met15
34	Apigenin 7-O-(3′′-O-Acetyl)-B-D-Glucuronide ($C_{23}H_{20}O_{12}$)	-	-5.77	59.26	Asp214, Ser218, Gly216	Ile123, Tyr77
35	Quercetin ($C_{15}H_{10}O_7$)	5280343	-6.41	19.99	Tyr77	Trp41, Phe111, Ile123, Met75, Val82

Fig. 2 showed that fredericone B, isophytol and quercetin have a hydrogen interaction with ASP34 and the same hydrophobic interactions with the plasmepsin II's native ligand.

Lipinski's rule of five (Ro5) in this study was calculated with the pKCSM predictor shown in table 2.

The pharmacokinetic predictions of the compounds were carried out using the pkCSM program and ADMETlab 2.0 with the parameters of Caco-2, human intestinal absorption (HIA), plasma protein binding (PPB), and Ames toxicity. The results of pharmacokinetic prediction are shown in table 3.

A molecular dynamics (MD) simulation was conducted for the selected compounds, namely fredericone B, isophytol, quercetin, and artemisinin, as a controlled drug using the AMBER16 program. Ligand and receptor parametrization was performed using ff14SB, GAFF force file, and AM1-BCC [25]. The results can be designated using RMSD and RMSF values. The RMSD and RSMF value of the compounds-2IGY complex during 20 ns MD is showed in fig. 3 and fig. 4.

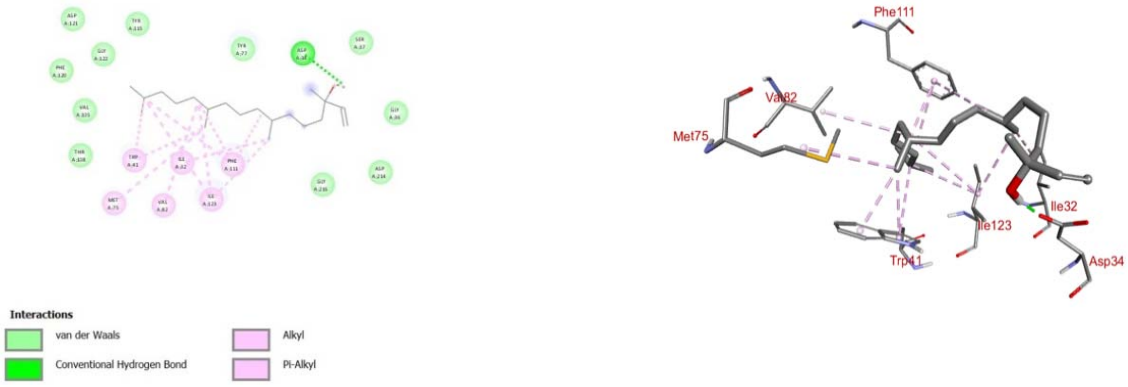

(a)

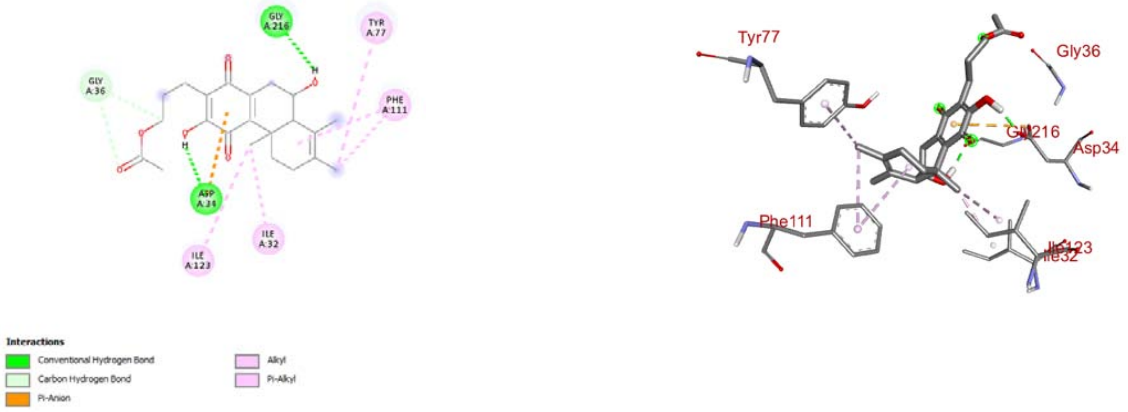

(b)

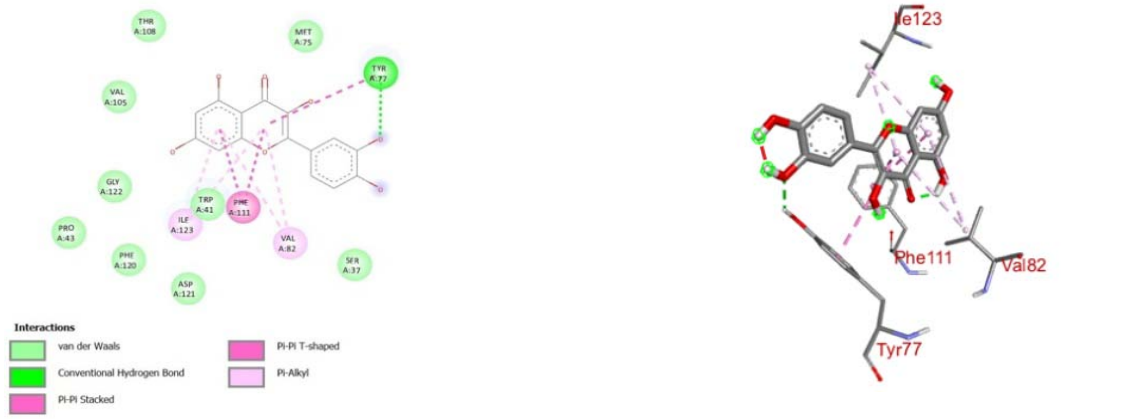

(c)

Fig. 2: The 2D and 3D visualization of docking results (a) isophytol; (b fredericone B); (c) quercetin

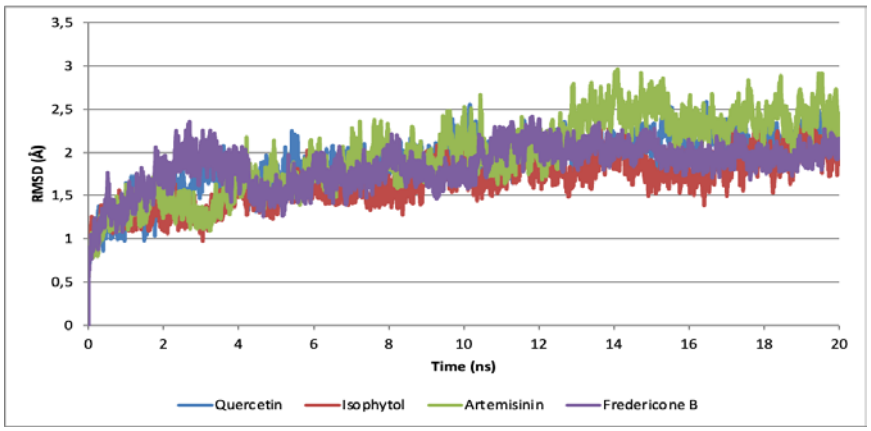

Fig. 3: The RMSD value of the compounds-2IGY complex during 20 ns MD

Table 2: Screening of ligand-based drug likeness (drug scan of miana leaf compounds)

No.	Compounds	Parameters			
		Molecular weight (≤500 g/mol)	Log P (≤5)	H-bond	
				Donor (≤5)	Acceptor (≤10)
	Artemisinin	282.33	-3.42	0	5
1	Neomenthol	156.27	2.43	1	1
2	Linalool	154.25	2.66	1	1
3	Germacrene-d	204.35	4.89	0	0
4	Neophytadiene	278.52	7.16	0	0
5	Delta-cadinene	204.35	4.72	0	0
6	Alpha-humulene	204.35	5.03	0	0
7	6, 10, 14-trimethyl-2-pentadecanone	268.48	6.01	0	1
8	Copaene	204.35	4.27	0	0
9	Cariophyllene oxide	220.35	3.93	0	1
10	Alpha-selinene	204.35	4.72	0	0
11	Alpha-cadinol	222.37	3.77	1	1
12	Beta-Sesquiphellandrene	204.35	4.89	0	0
13	Aromadendrene	204.35	4.27	0	0
14	Nerolidol	222.37	4.39	1	1
15	Alpha-calacorene	200.32	4.54	0	0
16	Torreyol	222.37	3.77	1	1
17	Alpha-Cubebene	204.35	4.27	0	0
18	Beta-Caryophyllene	204.35	4.72	0	0
19	Isophytol	296.54	6.36	1	1
20	Spiroscutelone A	462.49	0.22	3	9
21	Spiroscutelone B	504.53	1.25	1	10
22	Spiroscutelone C	506.54	1.04	2	10
23	Scutellarioidone A	378.42	0.76	4	7
24	Scutellarioidone B	448.51	2.58	2	8
25	Scutellarioidone C	460.47	3.15	3	9
26	6-Acetylfredericone B	428.52	4.66	1	6
27	Scutellarioidone D	388.46	2.96	2	6
28	Scutellarioidolide A	490.59	4.68	0	8
29	Coleon O	388.46	1.88	2	6
30	Coleon G	388.46	1.74	2	6
31	Lanugone K	406.51	2.59	2	6
32	Fredericone B	388.46	3.10	2	6
33	Apigenin 5-O-(3′′-O-Acetyl)-B-D-Glucuronide	488.40	0.71	5	11
34	Apigenin 7-O-(3′′-O-Acetyl)-B-D-Glucuronide	488.40	0.71	5	11
35	Quercetin	302.24	1.98	5	7

Table 3: Pharmacokinetics prediction of miana leaf compounds

No.	Compounds	Parameters			
		HIA (%)	Caco-2 (10^{-6} cm/s)	PPB (%)	Ames toxicity
	Artemisinin	97.543	1.295	71.637	Yes
1	Neomenthol	95.257	1.376	82.256	No
2	Linalool	93.163	1.493	85.370	No
3	Germacrene-d	95.590	1.436	97.456	No
4	Neophytadiene	92.850	1.425	98.552	No
5	Delta-cadinene	96.128	1.422	97.303	No
6	Alpha-humulene	94.682	1.421	93.024	No
7	6, 10, 14-trimethyl-2-pentadecanone	93.658	1.524	98.255	No
8	Copaene	96.221	1.374	97.259	No
9	Cariophyllene oxide	95.421	1.509	86.241	No
10	Alpha-selinene	94.127	1.401	94.702	No
11	Alpha-cadinol	94.296	1.479	96.719	No
12	Beta-sesquiphellandrene	94.668	1.408	98.065	No
13	Aromadendrene	95.302	1.395	93.569	No
14	Nerolidol	91.887	1.498	92.522	No
15	Alpha-calacorene	95.296	1.55	95.662	No
16	Torreyol	94.296	1.479	96.371	No
17	Alpha-Cubebene	95.964	1.389	96.371	No
18	Beta-Caryophyllene	94.845	1.423	95.289	No
19	Isophytol	91.304	1.517	98.741	No
20	Spiroscutelone A	79.434	0.575	44.315	No
21	Spiroscutelone B	84.057	0.847	46.304	No
22	Spiroscutelone C	78.773	0.451	34.670	No
23	Scutellarioidone A	57.414	0.275	67.372	No
24	Scutellarioidone B	68.423	0.926	95.895	Yes
25	Scutellarioidone C	90.518	0.866	91.100	No
26	6-Acetylfredericone B	95.281	1.055	93.550	No

No.	Compounds	Parameters			
		HIA (%)	Caco-2 (10^{-6} cm/s)	PPB (%)	Ames toxicity
27	Scutellarioidone D	75.346	1.009	97.935	No
28	Scutellarioidolide A	96.314	0.902	81.446	No
29	Coleon O	87.450	1.092	77.225	Yes
30	Coleon G	66.524	0.513	92.024	No
31	Lanugone K	73.458	1.149	77.791	No
32	Fredericone B	83.743	0.948	97.935	No
33	Apigenin 5-O-(3''-O-Acetyl)-B-D-Glucuronide	27.879	-0.59	86.964	No
34	Apigenin 7-O-(3''-O-Acetyl)-B-D-Glucuronide	29.709	-0.46	89.587	No
35	Quercetin	77.207	-0.22	95.496	No

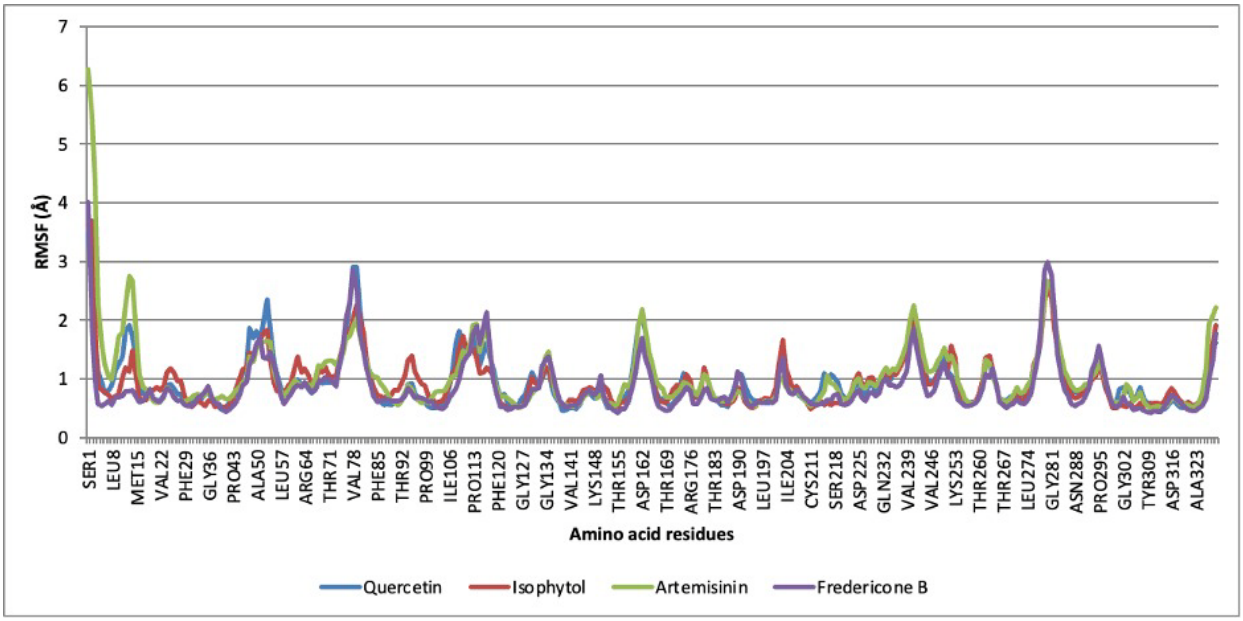

Fig. 4: The RMSF curve during 20 ns MD simulation for the compounds-2IGY complex

MM-GBSA (*Molecular Mechanics-Generalized Born Surface Area*) can calculate complex energy, producing a free energy value (ΔG) from the ligand-receptor system bond in molecular dynamics simulation, as shown in table 4.

Table 4: Binding free energy (ΔG) from the ligand-receptor system bond in the simulation of molecular dynamics

No	Energy components (kcal/mol)	Plasmepsin II			
		Quercetin	Isophytol	Artemisinin	Fredericone B
1	Van der Waals Interaction (VdW)	-17.6514	-36.1602	-1.2001	-24.8298
2	Electrostatic Energy(EEL)	335.9923	515.6917	294.3021	517.5085
3	Electrostatic Contribution to Solvation-Free Energy (EGB)	-325.95	-505.57	-292.1252	-493.0509
4	Non-polar Contribution to Solving Free Energy (ESURF)	-2.3125	-5.2864	-0.1365	-3.7071
5	ΔGgass (VdW+EEL)	318.3408	479.5315	293.1021	492.6788
6	ΔGsolv (EGB+ESURF)	-328.262	-510.856	-292.2617	-496.758
7	ΔGTOTAL (VdW+EEL+EGB+ESURF)	-9.9214	-31.3249	0.8403	-4.0793

DISCUSSION

In molecular docking, validation is needed by redocking the receptor with its native ligand. The validation parameter used is the RMSD value. RMSD less than 2.0 Å indicates the good reproducing quality of the binding pose [26,27]. The redocking validation of the 21GY receptor with the A2T ligand yielding an RMSD value of 0.872 Å (less than 2 Å) means the redocking was valid and shows similarities in the distance and the best ligand conformation in the redocking simulation with the distance and initial ligand conformation.

Molecular docking of 35 miana leaf compounds had free binding energy (ΔG) ranging from-4.48 to-8.09 at the plasmepsin II receptor. The more negative the free binding energy (FBE), the more stable it is. As a result, the ligand-protein affinity improves, leading to better activity [28]. The binding affinity is directly proportional to the Ki value, and the Ki value gives an idea of the compound's ability in an enzyme. The smaller the value of Ki, the greater the compound has pharmacological abilities in smaller doses [29].

It was shown in table 1 that germacrene D, delta-cadinene, copaene, alpha selinene, beta-sesquiphellandrene, aromadendrene, alpha-calacorene, isophytol, spiroscutelone A, coleon G, and fredericone B have a lower FBE value than artemisinin. Copaene has the lowest FBE for plasmepsin II receptors among the terpenoid-tested ligands. Still, it has no hydrogen interaction with the plasmepsin II receptor's crucial amino acid residue, ASP34, so the bond between copaene and plasmepsin II is thought to be less stable [10]. The more the ligand binds to the receptor amino acid, the closer the distance between them and the more stable it is. The distance in hydrogen bonds is much closer than in hydrophobic interactions. The presence of hydrogen can affect the chemical-physical properties of a drug so that it plays an essential role in the biological activity of the drug. In comparison, this hydrophobicity indicates the degree of solubility of

the drug in the cell membrane, which is predicted to affect the receptor's active site [10, 29].

The fredericone B and isophytol have a lower FBE than artemisinin as drug control, so it can be predicted that among the terpenoids tested ligands, fredericone B and isophytol have the best interaction with plasmepsin II (2IGY). Among the flavonoids tested ligands, quercetin has the lowest FBE (-6.41 kcal/mol), lower than artemisinin. The quercetin has a hydrogen interaction with plasmepsin II but in the amino acid residue Tyr77 and the same hydrophobic interactions with the receptor's native ligand (Trp41, Phe111).

The docking results showed a good interaction between flavonoid (quercetin) and terpenoid (fredericone B and isophytol) derived from miana leaves. Several flavonoid and terpenoid compounds from other plants also produce good interactions with Plasmepsin II. Previous research in some journals shows that the bond between Plasmepsin II and gingerol derived from ginger rhizome interacts well with the lowest free binding energy compared to the interaction of Plasmepsin II with several compounds derived from Indonesian spice plants. Several flavonoid compounds such as cyanidin 3,5-di-(6-malonylglucoside); isoscutellarein 4'methyl ether 8-(6"-n-butylglucuronide); cyanidin 3-(6"-malonylglucoside)-5-glucoside; delphinidin 3-(2-rhamnosyl-6-malonylglucoside); cyanidin 3-[6-(6-sinapylglucosyl)-2-xylosylgalactoside; delphinidin 3-(6-malonylglucoside)-3',5'-di-(6-p-coumaroylglucoside) and terpenoid compounds such as lycopene also provides low free energy binding and is thought to bind spontaneously to the plasmepsin II receptor [30, 31].

Lipinski's rule is considered for active compounds that are administered orally. The parameters of the Lipinski rule are the initial stage in determining the oral bioavailability of the active substance because it is related to the acceptance of the solubility and permeability of compounds in the gastrointestinal tract [32]. The test compound must comply with Lipinski's rules with no more than one violation. The rules must be met: hydrogen bond donor≤ 5, hydrogen bond acceptor ≤ 10, molecular weight ≤ 500 Da, and logP ≤ 5 [33]. Most of the test compounds met the requirements, accepting apigenin 5-O-(3′′-O-acetyl)-B-D-glucuronide and apigenin 7-O-(3′′-O-acetyl)-B-D-glucuronide. Thus, most of these compounds can be investigated further to determine their absorption, distribution, metabolism, and toxicity profiles.

HIA values indicate the degree of absorption of the active substance in the human intestine. A compound is categorized as well absorbed if the % HIA value is in the 70-100% range, sufficient in the 20-70% range, and poor in the 0-20% range [34]. Table 3 showed that scutellarioidone A, scutellarioidone B, coleon G, apigenin 5-O-(3′′-O-acetyl)-B-D-glucuronide, and apigenin 7-O-(3′′-O-acetyl)-B-D-glucuronide have poor ability to be absorbed in the body because they have HIA parameter values in the range of 20-70%. In contrast, other compounds can be well absorbed in the body.

Caco-2 cell modeling was used to predict the absorption of the active substance via the oral route *in vitro*. In the pkCSM predictive model, the high permeability of Caco-2 cells has a value>0.9 x 10^{-6} cm/s. Based on table 3, it can be seen the most of the tested secondary metabolites of miana leaves have a high ability to penetrate the membrane. Isophytol and fredericone B, which have good interaction with the plasmepsin II receptor, have a good ability to penetrate cells. The ability of the compound to penetrate cells was essential to reach the target tissue so that it could provide activity [28].

Plasma Protein Binding (PPB) values influence the drug's pharmacokinetic and pharmacodynamic properties. The PPB value greater than 90% indicates that the drug is firmly bound to plasma proteins. In contrast, the PPB value of less than 90% suggests that the drug is weakly bound to plasma proteins, allowing it to be efficiently distributed to its target of action. [35]. Most of the miana's compounds tested in this research are firmly bound to plasma proteins, and only thirteen compounds: neomenthol, linalool, caryophyllene oxide, spiroscutelone A, spiroscutelone B, spiroscutelone C, scutellarioidone A, scutellarioidolide A, coleon O, lanugone K, apigenin 5-O-(3′′-O-Acetyl)-B-D-glucuronide, apigenin 7-O-(3′′-O-Acetyl)-B-D-glucuronide have PPB values<90%, this indicates that they focus on plasma proteins and have an excellent ability to support the body.

The toxicity prediction was made using the AMES test. AMES test is widely used to assess the mutagenic potential of a compound in bacteria. In the pkCSM predictive model, a positive test indicates that the compound is mutagenic and can act as a carcinogen. Most secondary metabolites of miana leaves were negative for the Ames test.

The molecular interactions between isophytol, fredericone B, and quercetin and the receptors are shown by hydrogen bonding and hydrophobic interactions. The isophytol, fredericone B, and quercetin complied with Lipinski rules, had good pharmacokinetic profiles and were not mutagenic and carcinogenic in the AMES Toxicity test.

The results of the molecular dynamic simulation can be designated using RMSD and RMSF values. RMSD analysis revealed that the receptor remains stable and is not denatured. The increasing fluctuation indicates that the protein structure is starting to open, and the fluctuation's stability suggests that the ligand has found a stable conformation to bind to the protein. Ligand-receptor interactions in Molecular Dynamics Simulation within 20 ns can be seen through the RMSD (Root Mean Square Deviation) graph. RMSD compares molecules' shifts or conformational changes during the simulation process. The RMSD value from the molecular dynamic of fredericone B, isophytol, quercetin, and artemisinin showed the interaction of the plasmepsin II receptor (2IGY) with quercetin has a better stability than Isophytol and Artemisinin compounds as comparison drugs. Quercetin and isophytol have the same RMSD value (+1.85 Å), but quercetin tends to be stable from 4 ns, but isophytol quercetin tends to be stable from 9 ns. Fredericone B tends to be stable from 15 ns with an RMSD value (+2 Å). These RSMD values showed that quercetin is predicted to have the most stable interaction ability with plasmepsin receptors among the three compounds.

The Root Mean Square Fluctuation (RMSF) describes the flexibility of amino acid residues. The RMSF is calculated for each residue that makes up the protein to see how much fluctuation in each residue's movement occurs during the simulation. The RMSF is calculated for each residue that makes up the protein to see how much fluctuation in each residue's movement occurs during the simulation. A low RMSF value indicates low flexibility, produces a stable interaction, and plays an active role in the ligand-receptor binding site. Meanwhile, if the RMSF value is high, which means increased flexibility, the interaction is unstable because it might have many changes in position during molecular dynamics simulations.

Theoretically, the plasmepsin II receptor binds to its native ligand through the amino acid residue Asp34. Fig. 4 shows that all residues fluctuate in the same region. This is related to the fact that the amino acid residue Asp34 gives a reasonably low fluctuation in both isophytol and quercetin compounds and is also common in artemisinin. The most considerable fluctuation occurs in the Ser1 amino acid residues in all tested compounds to 2IGY complexes.

The mm-GBSA calculation results indicate that isophytol has the most negligible value of total binding free energy, which means that the compound's ability to bind to the plasmapepsin II receptor is immense, quercetin and fredericone B also has a lower total binding free energy than artemisinin, so it has an excellent ability to bond to the receptor. While artemisinin has the most significant total binding free energy value, so among tested ligands, it has the worst ability to bind to plasmepsin II protein.

CONCLUSION

The results of a computational approach to the interaction of 35 miana leaf compounds against plasmepsin II protein (2IGY) showed that isophytol, fredericone B and quercetin have the best interaction with plasmepsin II receptors. Isophytol (-6.45 kcal/mol), fredericone B (-6,87 kcal/mol) and quercetin (-6.41 kcal/mol) have a lower binding affinity than artemisinin (control drug). The results of the molecular dynamics of the compound at 20 ns predicted that

isophytol and quercetin have more stable interactions with plasmepsin II (2IGY), but Isophytol has the lowest total binding free energy from the ligand-receptor system bound in the molecular dynamics simulations, so isophytol can be expected to be useful as an antimalarial candidate from miana leaves.

FUNDING

Nil

AUTHORS CONTRIBUTIONS

All the authors have contributed equally.

CONFLICT OF INTERESTS

No conflicts of interest

REFERENCES

1. WHO. WHO guidelines for malaria. World Health Organization; 2021. http://apps.who.int/iris.
2. Rosenthal PJ. Antiprotozoal drugs. In: Katzung BG. editor Basic and Clinical Pharmacology. 14th ed. McGraw-Hill Education; 2017. p. 917-37.
3. Ippolito MM, Moser KA, Kabuya JBB, Cunningham C, Juliano JJ. Antimalarial drug resistance and implications for the WHO global technical strategy. Curr Epidemiol Rep. 2021;8(2):46-62. doi: 10.1007/s40471-021-00266-5, PMID 33747712.
4. Foley M, Tilley L. Quinoline antimalarials: mechanisms of action and resistance and prospects for new agents. Pharmacol Ther. 1998;79(1):55-87. doi: 10.1016/s0163-7258(98)00012-6, PMID 9719345.
5. Penna Coutinho J, Cortopassi WA, Oliveira AA, França TCC, Krettli AU. Antimalarial activity of potential inhibitors of Plasmodium falciparum lactate dehydrogenase enzyme selected by docking studies. PLOS ONE. 2011;6(7):e21237. doi: 10.1371/journal.pone.0021237, PMID 21779323.
6. Vennerstrom JL, Nuzum EO, Miller RE, Dorn A, Gerena L, Dande PA. 8-aminoquinolines active against blood-stage Plasmodium falciparum *in vitro* inhibit hematin polymerization. Antimicrob Agents Chemother. 1999;43(3):598-602. doi: 10.1128/AAC.43.3.598, PMID 10049273.
7. Meyers MJ, Goldberg DE. Recent advances in plasmepsin medicinal chemistry and implications for future antimalarial drug discovery efforts. Curr Top Med Chem. 2012;12(5):445-55. doi: 10.2174/156802612799362959, PMID 22242846.
8. Nasamu AS, Polino AJ, Istvan ES, Goldberg DE. Malaria parasite plasmepsins: more than just plain old degradative pepsins. J Biol Chem. 2020;295(25):8425-41. doi: 10.1074/jbc.REV120.009309, PMID 32366462.
9. Bhaumik P, Gustchina A, Wlodawer A. Structural studies of vacuolar plasmepsins. Biochim Biophys Acta. 2012;1824(1):207-23. doi: 10.1016/j.bbapap.2011.04.008, PMID 21540129.
10. Boss C, Richard Bildstein S, Weller T, Fischli W, Meyer S, Binkert C. Inhibitors of the Plasmodium falciparum parasite aspartic protease plasmepsin II as potential antimalarial agents. Curr Med Chem. 2003;10(11):883-907. doi: 10.2174/0929867033457674, PMID 12678679.
11. Cheuka PM, Dziwornu G, Okombo J, Chibale K. Plasmepsin inhibitors in antimalarial drug discovery: medicinal chemistry and target validation (2000 to present). J Med Chem. 2020;63(9):4445-67. doi: 10.1021/acs.jmedchem.9b01622, PMID 31913032.
12. Henderson JA, Shen J. Exploring the pH- and ligand-dependent flap dynamics of malarial plasmepsin II. J Chem Inf Model. 2022;62(1):150-8. doi: 10.1021/acs.jcim.1c01180, PMID 34964641.
13. Lisdawati V, Mutiatikum D, Alegantina SNY. Karakterisadi daun miana (Plectranthus scutellarioides (L.) BTH.) dan buah sirih (Piper betle L.) secara fisiko kimia dari ramuan lokal antimalaria daerah Sulawesi Utara. Media Health Res Dev. 2008;18.
14. Tjitraresmi A, Moektiwardoyo M, Susilawati Y, Shiono Y. Antimalarial activity of lamiaceae family plants. Syst Rev Pharm. 2020;11(7):324-33.
15. Cretton S, Saraux N, Monteillier A, Righi D, Marcourt L, Genta Jouve G. Anti-inflammatory and antiproliferative diterpenoids from Plectranthus scutellarioides. Phytochemistry. 2018;154:39-46. doi: 10.1016/j.phytochem.2018.06.012, PMID 29960256.
16. Kubinova R, Gazdova M, Hanakova Z, Jurkaninova S, Dall'Acqua S, Cvacka J. New diterpenoid glucoside and flavonoids from Plectranthus scutellarioides (L.) R. Br. S Afr J Bot. 2019;120:286-90. doi: 10.1016/j.sajb.2018.08.023.
17. Ito T, Rakainsa SK, Nisa K, Morita H. Three new abietane-type diterpenoids from the leaves of Indonesian Plectranthus scutellarioides. Fitoterapia. 2018;127:146-50. doi: 10.1016/j.fitote.2018.02.013, PMID 29447983.
18. Mustarichie R, Moektiwardoyo M, Dewi WA. Isolation, identification, and characteristic of essential oil of iler (Plectranthus scutellarioides (L.) R. Br leaves. J Pharm Sci Res. 2017;9(11):2218-23.
19. Dorr OS, Zimmermann BF, Kogler S, Mibus H. Influence of leaf temperature and blue light on the accumulation of rosmarinic acid and other phenolic compounds in Plectranthus scutellarioides (L.). Environ Exp Bot. 2019;167(June):103830. doi: 10.1016/j.envexpbot.2019.103830.
20. Moektiwardoyo M, Levita J, Sidiq SP, Ahmad K, Subarnas A, Java W. The determination of quercetin in Plectranthus scutellarioides (L.) R. Br. leaves extract and its *in silico* study on histamine H4 receptor penentuan kuersetin dari ekstrak metanol daun jawer. Majalah Farmasi Indones. 2011;22(3):191-6.
21. Ruswanto R, Mardianingrum R, Siswandono S, Kesuma D. Reverse docking, molecular docking, absorption, distribution, and toxicity prediction of artemisinin as an anti-diabetic candidate. Molekul. 2020;15(2):88. doi: 10.20884/1.jm.2020.15.2.579.
22. Chaniad P, Mungthin M, Payaka A, Viriyavejakul P, Punsawad C. Antimalarial properties and molecular docking analysis of compounds from Dioscorea bulbifera L. as new antimalarial agent candidates. BMC Complement Med Ther. 2021;21(1):144. doi: 10.1186/s12906-021-03317-y, PMID 34006257.
23. Lipinski CA, Lombardo F, Dominy BW, Feeney PJ. Experimental and computational approaches to estimate solubility and permeability in drug discovery and development settings. Adv Drug Deliv Rev. 2001;46(1-3):3-26. doi: 10.1016/s0169-409x(00)00129-0. PMID 11259830.
24. Case DA, Cheatham TE, Darden T, Gohlke H, Luo R, Merz KM. The amber biomolecular simulation programs. J Comput Chem. 2005;26(16):1668-88. doi: 10.1002/jcc.20290, PMID 16200636.
25. Mardianingrum R, Yusuf M, Hariono M, Mohd Gazzali A, Muchtaridi M. α-mangostin and its derivatives against estrogen receptor alpha. J Biomol Struct Dyn. 2022;40(6):2621-34. doi: 10.1080/07391102.2020.1841031, PMID 33155528.
26. Musfiroh I, Septiandi I, Megantara S, Tjitraresmi A, Muchtaridi. Interaction analysis of Asiatic acid and its derivatives to three isozyme of nitric oxide synthase (NOS) using molecular docking. Res J Chem Environ. 2019;23(12).
27. Shoichet BK, McGovern SL, Wei B, Irwin JJ. Lead discovery using molecular docking. Curr Opin Chem Biol. 2002;6(4):439-46. doi: 10.1016/s1367-5931(02)00339-3, PMID 12133718.
28. Subramanian G, Kitchen DB. Computational approaches for modeling human intestinal absorption and permeability. J Mol Model. 2006;12(5):577-89. doi: 10.1007/s00894-005-0065-z, PMID 16583199.
29. Trott O, Olson AJ. AutoDock Vina: improving the speed and accuracy of docking with a new scoring function, efficient optimization, and multithreading. J Comput Chem. 2010;31(2):455-61. doi: 10.1002/jcc.21334, PMID 19499576.
30. Malau ND. Antimalarial activity in plasmepsin II inhibitors using molecular docking. Int J Prog Sciences Technol. 2021;7(1):111-20.
31. Chaturvedi P, Raina V, Solanki PS, Saxena VL. *In silico* prediction of the anti-plasmodial activity of spices: targeting malarial proteases. J Clin Diagn Res. 2019;13(8):1-6. doi: 10.7860/JCDR/2019/34534.13035.
32. Ramachandran B, Kesavan S, Rajkumar T. Molecular modeling and docking of small molecule inhibitors against NEK2. Bio information. 2016;12(2):62-8. doi: 10.6026/97320630012062, PMID 28104962.

33. Lipinski CA. Lead- and drug-like compounds: the rule-of-five revolution. Drug Discov Today Technol. 2004;1(4):337-41. doi: 10.1016/j.ddtec.2004.11.007, PMID 24981612.
34. Cheng F, Li W, Liu G, Tang Y. *In silico* ADMET prediction: recent advances, current challenges and future trends. Curr Top Med Chem. 2013;13(11):1273-89. doi: 10.2174/15680266113139990033, PMID 23675935.
35. Purwaniati P. Molecular docking study on COVID-19 drug activity of N-(2-phenylethyl) methanesulfonamide derivatives as main protease inhibitor. Addawaa J Pharm Sci. 2020;3(1). doi: 10.24252/djps.v3i1.13945.